

From a PGeP Pincer-Type Germylene to Metal Complexes Featuring Chelating (Ir) and Tripodal (Ir) PGeP Germyl and Bridging (Mn₂) and Chelating (Ru) PGeP Germylene Ligands

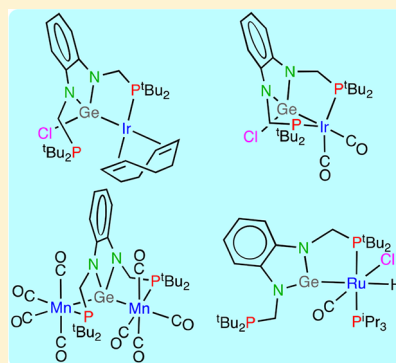
Javier Brugos,[†] Javier A. Cabeza,^{*,†} Pablo García-Álvarez,[†] and Enrique Pérez-Carreño[‡]

[†]Centro de Innovación en Química Avanzada (ORFEO-CINQA), Departamento de Química Orgánica e Inorgánica, Universidad de Oviedo, 33071 Oviedo, Spain

[‡]Departamento de Química Física y Analítica, Universidad de Oviedo, 33071 Oviedo, Spain

S Supporting Information

ABSTRACT: Different coordination modes of a PGeP chloridogermyl ligand (*Ge,P*-chelating and *P,Ge,P*-tripodal) and a PGeP germylene ligand (*P,Ge,P*-bridging and *Ge,P*-chelating) have been identified in coordination compounds resulting from reactions of the PGeP pincer-type diphosphane-germylene $\text{Ge}(\text{NCH}_2\text{P}^t\text{Bu}_2)_2\text{C}_6\text{H}_4$ (**1**) with iridium(I), manganese(0), and ruthenium(II) complex reagents. Germylene **1** reacted with $[\text{Ir}_2(\mu\text{-Cl})_2(\eta^4\text{-cod})_2]$ ($\text{cod} = 1,5\text{-cyclooctadiene}$) to give $[\text{Ir}\{\kappa^2\text{Ge,P-GeCl}(\text{NCH}_2\text{P}^t\text{Bu}_2)_2\text{C}_6\text{H}_4\}(\eta^4\text{-cod})]$ (**2**), which contains a *Ge,P*-chelating PGeP chloridogermyl ligand and an uncoordinated phosphane group that weakly interacts with the Ge atom. Carbon monoxide readily displaced the cod ligand of **2** to give the dicarbonyl derivative $[\text{Ir}\{\kappa^3\text{P,Ge,P-GeCl}(\text{NCH}_2\text{P}^t\text{Bu}_2)_2\text{C}_6\text{H}_4\}(\text{CO})_2]$ (**3**), in which the PGeP chloridogermyl ligand displays a *P,Ge,P*-tripodal coordination mode. A bridging germylene moiety has been identified in the binuclear derivative $[\text{Mn}_2\{\mu\text{-}\kappa^3\text{P,Ge,P-Ge}(\text{NCH}_2\text{P}^t\text{Bu}_2)_2\text{C}_6\text{H}_4\}(\text{CO})_8]$ (**4**), which resulted from the treatment of $[\text{Mn}_2(\text{CO})_{10}]$ with germylene **1**. The ruthenium complex $[\text{RuHCl}(\text{CO})\{\kappa^2\text{Ge,P-Ge}(\text{NCH}_2\text{P}^t\text{Bu}_2)_2\text{C}_6\text{H}_4\}(\text{P}^t\text{Pr}_3)]$ (**5**), which was isolated from the reaction of **1** with $[\text{RuHCl}(\text{CO})(\text{P}^t\text{Pr}_3)_2]$, is the first transition-metal derivative of **1** in which the germylene moiety has not inserted into an M–M or M–Cl bond (M = transition metal), as it contains germylene **1** coordinated in a *Ge,P*-chelating mode, the resulting GeNCPRu ring being severely strained due to the short length of the coordinated $\text{CH}_2\text{P}^t\text{Bu}_2$ arm, which also forces the germanium atom to be in an uncommon T-shaped environment. DFT calculations have been used to shed light on bonding features of complexes **2** and **5**. The X-ray structures of **1**–**5** are also reported.



INTRODUCTION

The use of heavier carbene analogues, also called heavier tetrylenes, as ligands in transition-metal chemistry has increased a great deal in the past few years.¹ This intense research activity has been stimulated by their ambiphilic character (they can behave as Lewis bases and acids), by their strong electron-donating capacity (those that are donor-stabilized are even stronger electron donors than most phosphanes and N-heterocyclic carbenes²), and by the discovery that some of their complexes are efficient catalyst precursors for homogeneous catalytic transformations.^{3,4}

On the other hand, many efforts have also been devoted in the last two decades to the design and synthesis of pincer ligands comprising strong electron-donating groups because transition-metal complexes containing such ligands have been successfully used in many stoichiometric⁵ and catalytic reactions^{5,6} involving bond activation processes (strong electron-donating ligands facilitate the participation of their complexes in oxidative addition reactions⁷).

Despite the increasing interest in heavier tetrylenes and pincer ligands, very few pincer-type ligands (free or forming part of transition-metal complexes) have been reported to be

equipped with at least one heavier tetrylene as a donor group: Hahn and co-workers have described GeNGe and GeCGe pincers in which a pyridine-2,6-diyl or a benzene-1,3-diyl group, respectively, are linked to two 2-germabenzimidazol-2-ylidene fragments,⁸ and also the NSnN pincers $\text{Sn}\{\text{N}(\text{CH}_2)_n\text{NMe}_2\}_2\text{C}_6\text{H}_4$ ($n = 1, 2$),⁹ but their behavior as ligands has not been investigated; the Driess group has described the synthesis, some coordination chemistry, and catalytic applications of ECE^{10} and ENE^{11} pincers having benzamidinato-silylenes or -germylenes as E-donor groups; the groups of Whited,¹² Ozerov,¹³ and Zybail¹⁴ have reported some transition-metal complexes containing the PSiP pincers $\text{Si}(\text{C}_6\text{H}_4\text{PPh}_2)_2$,¹² $\text{Si}(\text{C}_6\text{H}_4\text{P}^t\text{Pr}_2)_2$,¹³ and $\text{Si}(\text{C}_6\text{H}_4\text{CH}_2\text{PPh}_2)_2$,¹⁴ respectively, but their syntheses used silanes instead of free silylenes; and we have recently communicated the synthesis and some transition-metal derivative chemistry of the metal-free pincer-type PGeP germylene $\text{Ge}(\text{NCH}_2\text{P}^t\text{Bu}_2)_2\text{C}_6\text{H}_4$ ^{15,16} and PSnP stannylene $\text{Sn}(\text{NCH}_2\text{P}^t\text{Bu}_2)_2\text{C}_6\text{H}_4$.¹⁷

Received: March 22, 2018

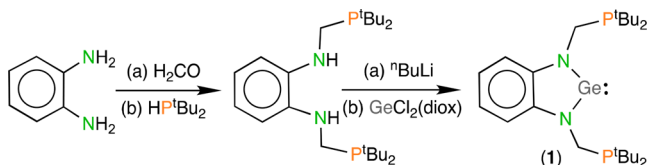


Our aforementioned studies on the reactivity of germylene $\text{Ge}(\text{NCH}_2\text{P}^t\text{Bu}_2)_2\text{C}_6\text{H}_4$ (**1**) with transition-metal complexes provided reaction products that resulted from the insertion of the Ge atom of **1** into Co–Co¹⁵ or M–Cl (M = Rh,¹⁵ Ni,¹⁶ Pd,¹⁶ Pt¹⁶) bonds, but in no instance did we obtain a product derived from the simple coordination (not insertion) of the germylene fragment to a metal atom. We now report the hitherto unknown X-ray diffraction (XRD) structure of germylene **1** and reactions of this PGeP pincer-type germylene with common iridium(I), manganese(0), and ruthenium(II) complexes affording transition-metal derivatives in which we have characterized chelating and tripodal PGeP germyl (Ir), bridging PGeP germylene (Mn_2), and unprecedented chelating PGeP germylene (Ru) ligands, the last also representing the first ruthenium complex to have a nondonor-stabilized N-heterocyclic germylene coordinated as a terminal ligand.

RESULTS AND DISCUSSION

XRD Structure of Germylene 1. At the time we communicated the synthesis of germylene **1** (Scheme 1),¹⁵ its

Scheme 1. Synthesis of Germylene 1



molecular structure could not be unambiguously determined. It was inferred from spectroscopic data and from DFT calculations. A subsequent in-depth DFT study on PEP tetrylenes of the type $\text{E}(\text{NCH}_2\text{P}^t\text{Bu}_2)_2\text{C}_6\text{H}_4$ (E = C, Si, Ge, Sn) concluded that the most stable conformation of the molecules with E = Ge, Sn has the lone pairs of both P atoms weakly interacting with empty orbitals with a large participation of the Ge atom, resulting in unexpectedly short separations between the E and P atoms, but this is not the case for the lighter tetrylenes (E = C, Si).¹⁷

After many attempts, we have now been able to crystallize germylene **1** and its molecular structure has finally been determined by XRD. Figure 1 confirms that **1** has C_2 symmetry and that the P atoms, which are almost in the plane defined by the atoms of the 2-germabenzimidazol-2-ylidene fragment, are only 3.320(2) Å away from the Ge atom, a distance that is 0.6 Å shorter than the sum of van der Waals radii of these elements.¹⁸ This structure is similar to that of the tin analogue $\text{Sn}(\text{NCH}_2\text{P}^t\text{Bu}_2)_2\text{C}_6\text{H}_4$, in which the $\text{Sn}\cdots\text{P}$ distances are 3.277(1) and 3.313(1) Å (in this case, the molecule is not symmetric).¹⁷

Iridium(I) Derivatives of Germylene 1. The iridium(I) dimer $[\text{Ir}_2(\mu\text{-Cl})_2(\eta^4\text{-cod})_2]$ (cod = 1,5-cyclooctadiene) reacted readily with germylene **1** (1:2 mole ratio) to give the chloridogermyl complex $[\text{Ir}\{\kappa^2\text{GeP-GeCl}(\text{NCH}_2\text{P}^t\text{Bu}_2)_2\text{C}_6\text{H}_4\}(\eta^4\text{-cod})]$ (**2**) as the only reaction product (Scheme 2).

An XRD study (Figure 2) confirmed the insertion of the Ge atom into an Ir–Cl bond and that the resulting PGeP chloridogermyl ligand is GeP -chelated to an $\text{Ir}(\eta^4\text{-cod})$ fragment. Therefore, the complex maintains an uncoordinated phosphane fragment. This feature was also suggested by the $^{31}\text{P}\{\text{H}\}$ NMR spectrum of **2**, which contains two uncoupled resonances at 75.9 (coordinated P) and 29.7 (free P) ppm. The

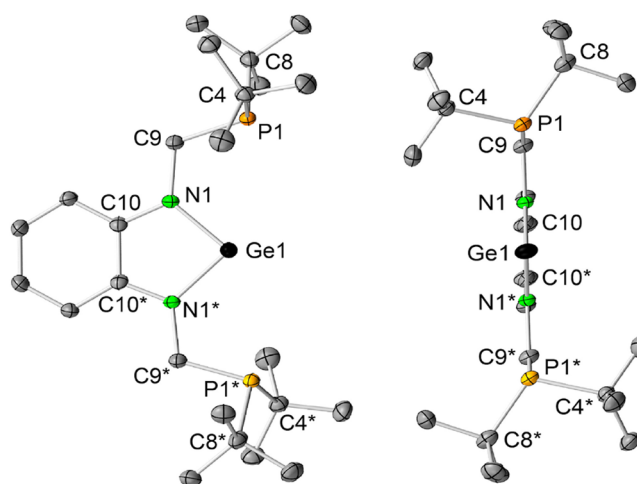
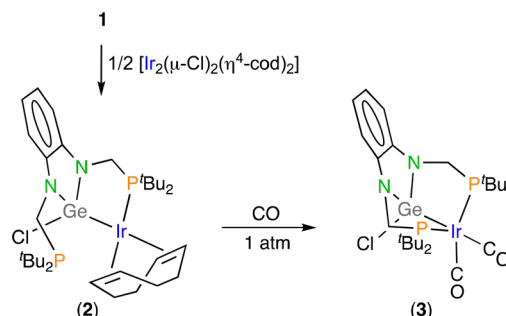


Figure 1. Two views of the XRD molecular structure of germylene **1** (35% displacement ellipsoids; H atoms omitted for clarity; atoms marked with asterisks are related to unmarked atoms by a C_2 symmetry axis). Selected interatomic distances (Å) and angles (deg): $\text{Ge1}\cdots\text{P1}$ 3.320(2), $\text{Ge1}\cdots\text{N1}$ 1.879(4), $\text{P1}\cdots\text{C4}$ 1.890(5), $\text{P1}\cdots\text{C8}$ 1.880(6), $\text{P1}\cdots\text{C9}$ 1.861(5), $\text{N1}\cdots\text{C9}$ 1.473(5), $\text{N1}\cdots\text{C10}$ 1.379(6), $\text{C10}\cdots\text{C10}^*$ 1.436(9); $\text{N1}\cdots\text{Ge1}\cdots\text{N1}^*$ 84.0(2).

Scheme 2. Synthesis of Complexes 2 and 3



Ir–Ge bond distance, 2.4275(3) Å, is comparable to those measured in other iridium(I) complexes containing germyl ligands.¹⁹ The insertion of nondonor-stabilized germylenes into Ir–Cl bonds has seldom been observed.²⁰ For comparison, it should be noted that the metal atoms of the related known PSiP silyl rhodium complexes $[\text{Rh}\{\kappa^3\text{P-Si-P-SiCl}(\text{C}_6\text{H}_4\text{PPh}_2)_2\}(\eta^4\text{-cod})]$ and $[\text{Rh}\{\kappa^3\text{P-Si-P-Si}(\text{OTf})(\text{C}_6\text{H}_4\text{PPh}_2)_2\}(\eta^4\text{-nbd})]$ (nbd = norbornadiene), which were respectively prepared from the silane $\text{H}_2\text{Si}(\text{C}_6\text{H}_4\text{PPh}_2)_2$ and $[\text{Rh}_2(\mu\text{-Cl})_2(\eta^4\text{-cod})_2]$ or $[\text{Rh}(\eta^4\text{-nbd})_2]\text{OTf}$, are pentacoordinated,²¹ probably because the smaller size of their phosphane groups allows a tridentate coordination of the corresponding PSiP silyl ligand in the presence of the η^4 -diene ligand.

A remarkable feature of the structure of complex **2** is that its uncoordinated P atom is in the proximity of the Ge atom, at a distance (3.361(2) Å) that is only 0.041 Å longer than that found in free germylene **1**. A similar structural feature has also been observed in the related rhodium complex $[\text{Rh}\{\kappa^2\text{GeP-GeCl}(\text{NCH}_2\text{P}^t\text{Bu}_2)_2\text{C}_6\text{H}_4\}(\eta^4\text{-cod})]$, in which the separation between the uncoordinated P atom and the Ge atom is 3.364(3) Å.¹⁵ Aiming at obtaining a rationale that could account for these structural observations, we performed a DFT study on complex **2**. An analysis of the NBO second-order perturbation donor–acceptor interactions revealed a non-negligible interaction, 12.3 kcal mol^{−1}, between the orbital

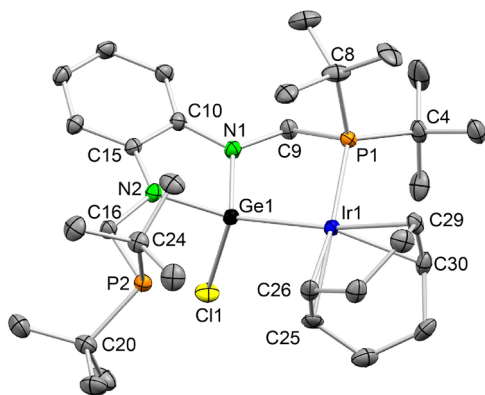


Figure 2. XRD molecular structure of complex **2** (35% displacement ellipsoids; H atoms omitted for clarity; only one of the two positions in which the methyl groups attached to C8 are disordered is shown). Selected bond distances (Å) and angles (deg): Ir1–C25 2.199(3), Ir1–C26 2.188(2), Ir1–C29 2.193(2), Ir1–C30 2.202(3), Ir1–P1 2.3652(6), Ir1–Ge1 2.4275(3), Ge1–N1 1.859(2), Ge1–N2 3.361(2), Ge1–N2 1.866(2), Ge1–Cl1 2.2806(7), P1–C4 1.888(3), P1–C8 1.903(3), P1–C9 1.865(2), P2–C16 1.854(2), P2–C20 1.890(3), P2–C24 1.890(3), N1–C9 1.430(3), N1–C10 1.374(3), N2–C15 1.399(3), N2–C16 1.451(3), C10–C15 1.421(4), C25–C26 1.395(4), C29–C30 1.402(4); P1–Ir1–Ge1 82.45(2), N1–Ge1–N2 85.78(9), N1–Ge1–Cl1 105.12(7), N2–Ge1–Cl1 99.15(7), N1–Ge1–Ir1 106.00(7), N2–Ge1–Ir1 142.04(6), Cl1–Ge1–Ir1 111.68(2).

that contains the lone pair of the uncoordinated P atom and the LUMO of the molecule, which is mainly contributed by the Ge atom and has a slight $\sigma^*(\text{Ge}-\text{N})$ character (Figure 3).

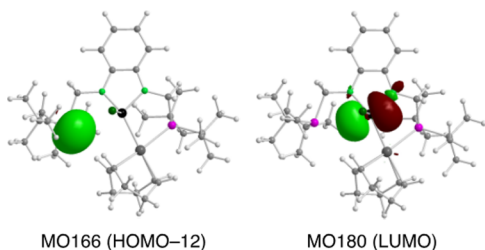


Figure 3. Filled (left) and empty (right) orbitals of complex **2** involved in the weak donor–acceptor interaction that accounts for the close proximity of the uncoordinated phosphane group to the Ge atom (NBO second-order perturbation donor–acceptor interaction analysis).

Analogous theoretical studies have shown that weak P...E (E = Ge, Sn) donor–acceptor interactions are also responsible for the most stable conformations of germylene **1**, its tin analogue, and also the ruthenium chloridostannyl complex $[\text{RuCl}(\kappa^2\text{Sn}, \text{P}-\text{SnCl}(\text{NCH}_2\text{P}^t\text{Bu}_2)_2\text{C}_6\text{H}_4)(\eta^6\text{-cym})]$ (cym = *p*-cymene).¹⁷

The dicarbonyl derivative $[\text{Ir}\{\kappa^3\text{P}, \text{Ge}, \text{P}-\text{GeCl}(\text{NCH}_2\text{P}^t\text{Bu}_2)_2\text{C}_6\text{H}_4\}(\text{CO})_2]$ (**3**) was quantitatively formed when a solution of complex **2** in toluene was exposed to a CO atmosphere (Scheme 2). Two strong ν_{CO} absorptions, at 2001 and 1956 cm^{-1} , were observed in the IR spectrum of the resulting solution; the low ν_{CO} values indicate that the metal atom is electron rich (the two phosphane fragments and the germyle ligand are strong electron donors). Its ^1H , $^{13}\text{C}\{^1\text{H}\}$, and $^{31}\text{P}\{^1\text{H}\}$ NMR spectra indicated mirror molecular symmetry (C_s), with the ^{31}P resonance appearing at a very high chemical shift, 116.3 ppm (in C_6D_6), suggesting a strained coordination

of both phosphane fragments (as has been previously observed in the PGeP pincer chloridogermyle square-planar metal derivatives $[\text{Rh}\{\kappa^3\text{P}, \text{Ge}, \text{P}-\text{GeCl}(\text{NCH}_2\text{P}^t\text{Bu}_2)_2\text{C}_6\text{H}_4\}(\text{CO})]$ ¹⁵ and $[\text{MCl}\{\kappa^3\text{P}, \text{Ge}, \text{P}-\text{GeCl}(\text{NCH}_2\text{P}^t\text{Bu}_2)_2\text{C}_6\text{H}_4\}]$ (M = Ni, Pd, Pt)).¹⁶ The XRD structure of complex **3** (Figure 4) confirmed

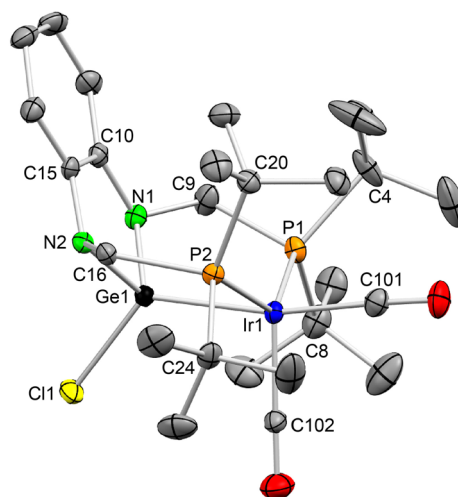


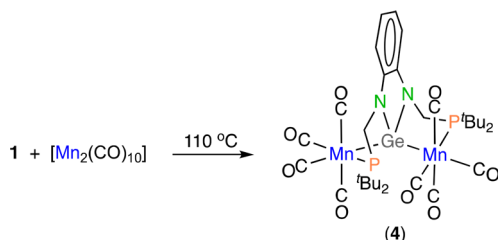
Figure 4. XRD molecular structure of complex **3** (30% displacement ellipsoids; H atoms omitted for clarity). Only one of the two analogous molecules found in the asymmetric unit is shown. Selected bond lengths (Å) and angles (deg): Ir1–C101 1.897(5), Ir1–C102 1.903(5), Ir1–P1 2.388(1), Ir1–P2 2.407(1), Ir1–Ge1 2.3880(5), Ge1–N1 1.865(4), Ge1–N2 1.856(4), Ge1–Cl1 2.203(1), P1–C4 1.889(6), P1–C8 1.899(6), P1–C9 1.880(5), P2–C16 1.899(5), P2–C24 1.900(5), P2–C20 1.908(5), N1–C9 1.454(7), N1–C10 1.399(6), N2–C15 1.402(6), N2–C16 1.454(6), C10–C15 1.415(7); C101–Ir1–P1 96.4(2), C101–Ir1–P2 95.6(2), C101–Ir1–Ge1 167.8(2), C101–Ir1–C102 97.2(2), C102–Ir1–P1 110.3(2), C102–Ir1–P2 112.3(2), C102–Ir1–Ge1 95.0(2), P1–Ir1–P2 133.66(4), P1–Ir1–Ge1 79.41(3), P2–Ir1–Ge1 79.63(3), N1–Ge1–N2 91.5(2), N1–Ge1–Cl1 107.5(1), N2–Ge1–Cl1 104.3(1), N1–Ge1–Ir1 112.0(1), N2–Ge1–Ir1 113.5(1), Cl1–Ge1–Ir1 123.22(4).

the tridentate coordination of the PGeP chloridogermyle ligand and the presence of two CO ligands on the iridium atom, which is in a distorted-trigonal-bipyramidal ligand environment with the Ge atom and a CO ligand in the axial positions. The observed distortion is caused by the short length of the $\text{CH}_2\text{P}^t\text{Bu}_2$ side arms, which does not allow the P atoms to reach the ideal equatorial plane of the bipyramid and forces the N atoms to be in a pyramidal environment (ideally, sp^2 -hybridized N atoms are trigonal planar). In contrast to complex **2**, in which the larger cod ligand only allows a bidentate coordination of the PGeP chloridogermyle ligand (see above), the smaller size of carbon monoxide allows a tridentate attachment of the PGeP chloridogermyle ligand in complex **3**. Given the nonplanarity of the GeP_2Ir atom grouping in **3**, the coordination type of its PGeP ligand can be referred to as “tripodal” rather than “pincer”. The stability of complex **3** toward CO loss confirms the higher disposition of iridium(I), in comparison to rhodium(I), to be pentacoordinate, since the reaction of the rhodium cod complex $[\text{Rh}\{\kappa^2\text{Ge}, \text{P}-\text{GeCl}(\text{NCH}_2\text{P}^t\text{Bu}_2)_2\text{C}_6\text{H}_4\}(\eta^4\text{-cod})]$ with CO gives a square-planar monocarbonyl PGeP pincer derivative.¹⁵

Reaction of Germylene **1 with $[\text{Mn}_2(\text{CO})_{10}]$.** The binuclear manganese(I) complex $[\text{Mn}_2\{\mu\text{-}\kappa^3\text{P}, \text{Ge}, \text{P}-\text{GeCl}(\text{NCH}_2\text{P}^t\text{Bu}_2)_2\text{C}_6\text{H}_4\}(\text{CO})_8]$ (**4**) was obtained from a reaction

in which a 1:1 mixture of $[\text{Mn}_2(\text{CO})_{10}]$ and germylene **1** was heated in toluene at reflux temperature for 4 h (Scheme 3).

Scheme 3. Synthesis of Complex 4



Mixtures of products that slowly evolved toward complex **4** were observed at shorter reaction times when the reaction was monitored by IR spectroscopy. After 4 h, the reaction mixture, which contained no $[\text{Mn}_2(\text{CO})_{10}]$, did not change with time and complex **4** was isolated in 56% yield after a chromatographic separation. The mass spectrum of **4** displayed the molecular ion, confirming its binuclear formulation. Its most informative NMR spectrum was the $^{31}\text{P}\{^1\text{H}\}$, which contained only one (rather broad) resonance with a high chemical shift of δ 142.7 ppm in CD_2Cl_2 , indicating that both P atoms are related by a symmetry element and that they are coordinated to manganese (whose only natural isotope, ^{55}Mn , has a nuclear spin of $I = 5/2$ and a quadrupolar moment, provoking broad NMR signals) in a strained arrangement (high chemical shift, see above).

The XRD structure of complex **4** (Figure 5) confirmed the insertion of the Ge atom of germylene **1** into the Mn–Mn bond of the original dimanganese(0) reagent and that each phosphane fragment is attached to a $\text{Mn}(\text{CO})_4$ unit, resulting in a binuclear complex of approximate (noncrystallographic) C_2 symmetry, with no metal–metal bond (the Mn...Mn distance is 4.5162(5) Å) and with both Mn atoms in an octahedral ligand

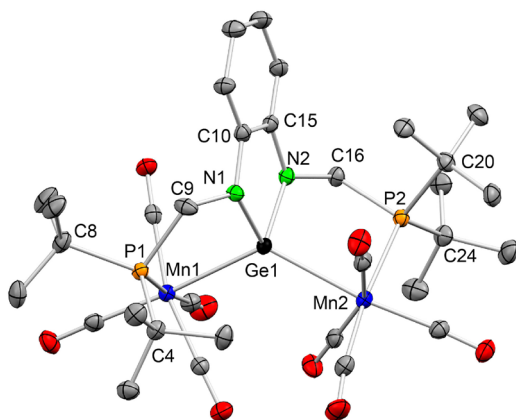
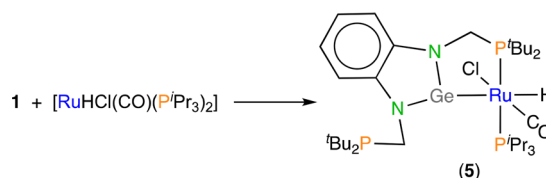


Figure 5. XRD molecular structure of complex **4** (35% displacement ellipsoids; H atoms omitted for clarity). Selected interatomic distances (Å) and angles (deg): Mn1...Mn2 4.5162(5), Mn1–Ge1 2.5127(5), Mn1–P1 2.3801(8), Mn2–Ge1 2.5615(5), Mn2–P2 2.3817(8), Ge1–N1 1.903(2), Ge1–N2 1.897(2), P1–C4 1.894(3), P1–C8 1.908(3), P1–C9 1.864(3), P2–C16 1.869(3), P2–C20 1.907(3), P2–C24 1.907(3), N1–C9 1.445(4), N1–C10 1.403(4), N2–C15 1.393(4), N2–C16 1.449(4), C10–C15 1.418(4); N1–Ge1–N2 85.4(1), N1–Ge1–Mn1 97.48(7), N2–Ge1–Mn1 117.54(7), N1–Ge1–Mn2 124.55(8), N2–Ge1–Mn2 99.99(7), Mn1–Ge1–Mn2 125.82(2).

environment. Some germylene-bridged dimanganese complexes are known, but they have not been prepared by germylene insertion into Mn–Mn bonds.²² Although the insertion of nondonor-stabilized germynes into other metal–metal bonds has been previously observed,^{15,23} the only hitherto reported complex that is structurally related to compound **4** is the dicobalt derivative $[\text{Co}_2\{\mu\text{-}\kappa^3\text{P}_2\text{GeP-Ge}(\text{NCH}_2\text{P}^i\text{Bu}_2)_2\text{C}_6\text{H}_4\}(\text{CO})_6]$, in which each Co atom is in a trigonal-bipyramidal environment.¹⁵

Reaction of Germylene 1 with $[\text{RuHCl}(\text{CO})(\text{P}^i\text{Pr}_3)_2]$. The coordinatively unsaturated ruthenium(II) complex $[\text{RuHCl}(\text{CO})(\text{P}^i\text{Pr}_3)_2]$, which has already shown a rich derivative chemistry,²⁴ reacted readily with germylene **1** to give $[\text{RuHCl}(\text{CO})\{\kappa^2\text{GeP}_2\text{Ge-Ge}(\text{NCH}_2\text{P}^i\text{Bu}_2)_2\text{C}_6\text{H}_4\}(\text{P}^i\text{Pr}_3)]$ (**5**) and free tris(isopropyl)phosphane (Scheme 4). Its spectro-

Scheme 4. Synthesis of Complex 5



scopic data indicated the absence of any symmetry, that the complex maintains the original hydride ($\delta_{\text{H}} -8.73$ ppm (dd, $J_{\text{HP}} = 21.6$ and 16.3 Hz)) and carbonyl (ν_{CO} 1916 (s) cm^{-1}) ligands, and that two of its three phosphane groups (δ_{P} 99.9 (d), 66.2 (d), 16.0 (s) ppm) are strongly coupled to each other ($J_{\text{PP}} = 243.0$ Hz), suggesting a mutually trans arrangement, but they did not help to unambiguously establish its molecular structure, which was determined by XRD (Figure 6).

Remarkably, in contrast with our initial expectation, compound **5** does not contain a chloridogermyl moiety. In fact, it is the first transition-metal derivative of compound **1** to have the germylene moiety not inserted into M–M or M–X (M = transition metal; X = halogen) bonds. Figure 6 shows that compound **5** is a hexacoordinate ruthenium(II) complex in which germylene **1** chelates the metal atom through the Ge atom and the P atom of one of its phosphane groups. As suggested by the $^{31}\text{P}\{^1\text{H}\}$ and ^1H NMR spectra, the two coordinated phosphane groups are trans to each other and cis to the hydride ligand, which is trans to the germylene moiety. The Ge,P-chelating attachment of ligand **1** to the Ru atom and the short length of the $\text{CH}_2\text{P}^i\text{Bu}_2$ arms do not allow the germylene fragment to coordinate in the expected symmetrical manner, provoking the GeNCPRu ring to be severely strained. Thus (a) although the Ru atom is in the plane of the 2-germabenzimidazol-2-ylidene moiety, it is almost aligned with a Ge–N bond ($\text{Ru1–Ge1–N2 } 166.5(2)^\circ$), with the Ge atom being in an unusual (almost) T-shaped environment, (b) the Ru1–P1 distance (2.413(2) Å) is notably longer than the Ru1–P3 distance (2.386(2) Å), and (c) the Ru–Ge bond length (2.434(1) Å), which cannot be compared with that of any ruthenium complex having a terminal nondonor-stabilized N-heterocyclic germylene ligand (such a complex has never been reported), is also much longer than that of $[\text{RuCl}\{\kappa^3\text{P}_2\text{GeP-GeCl}(\text{C}_6\text{H}_4\text{PPh}_2)_2\}(\text{PPh}_3)]$ (2.3906(5) Å), which contains a P,Ge,P-tripodal chloridogermyl ligand.²⁵ The very wide Ru1–Ge1–N2 angle of complex **5**, $166.5(2)^\circ$, is noteworthy because a search at the Cambridge Structural Database has revealed that the widest angle hitherto reported

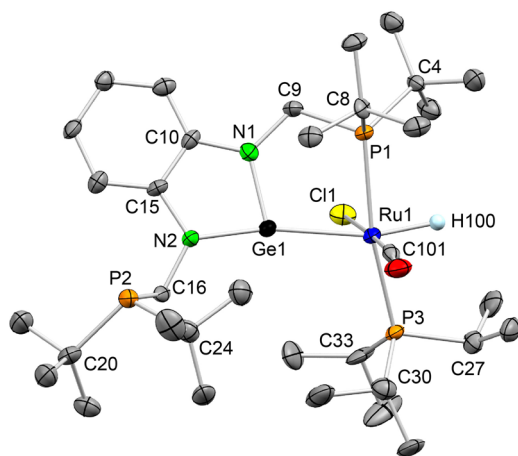


Figure 6. XRD molecular structure of complex **5** (35% displacement ellipsoids; H atoms, except the hydride ligand, omitted for clarity). Selected bond lengths (Å) and angles (deg): Ru1–C101 1.83(1), Ru1–Cl1 2.498(3), Ru1–P1 2.413(2), Ru1–P3 2.386(2), Ru1–Ge1 2.434(1), Ge1–N1 1.838(8), Ge1–N2 1.838(7), P1–C4 1.912(9), P1–C8 1.88(1), P1–C9 1.857(9), P2–C16 1.88(1), P2–C20 1.92(1), P2–C24 1.89(1), P3–C27 1.86(1), P3–C30 1.87(1), P3–C33 1.85(1), N1–C9 1.45(1), N1–C10 1.38(1), N2–C15 1.41(1), N2–C16 1.48(1), C10–C15 1.41(1); P1–Ru1–Ge1 81.06(6), P1–Ru1–Cl1 86.01(8), P1–Ru1–C101 95.9(3), P1–Ru1–P3 168.85(9), P3–Ru1–Ge1 108.11(7), P3–Ru1–Cl1 89.42(8), P3–Ru1–C101 89.0(3), Cl1–Ru1–Ge1 79.59(7), Cl1–Ru1–C101 177.3(3), C101–Ru1–Ge1 98.8(3), N1–Ge1–N2 86.2(3), N1–Ge1–Ru1 106.1(2), N2–Ge1–Ru1 166.5(2).

around a tricoordinate Ge atom is $159.8(1)^\circ$, found in $[\text{WHCl}\{\kappa^2\text{Ge}, P\text{-Ge}(\text{CH}_2\text{PMe}_2)\text{Ar}\}(\text{PMe}_3)_3]$ (Ar = 2,6-(trip) $_2\text{C}_6\text{H}_3$; trip = 2,4,6- $\text{Pr}_3\text{C}_6\text{H}_2$), which also features a chelating germylene-phosphane ligand.²⁶

As the asymmetric coordination of the germylene moiety of complex **5** differs considerably from the symmetric coordination found for other nondonor-stabilized germylenes, such as GeCl_2 ,²⁷ $\text{Ge}\{\text{N}(\text{SiMe}_3)_2\}_2$,^{19,23,28} and some cyclic germylenes,^{27,29} when they act as terminal ligands, we decided to undertake a molecular orbital study to investigate the bonding between the Ge and Ru atoms of complex **5**. The principal molecular orbital responsible for the Ge–Ru bond (NBO analysis) is the HOMO-86 (Figure 7), which has σ character, and its energy (-16.65 eV) is well below that of the HOMO (-7.56 eV). The large contribution of the undirected (spherical shape) Ge 4s atomic orbital to the HOMO-86 orbital of compound **5** (the composition of this orbital is given in the caption of Figure 7) implies that the overlap of the Ge lone pair orbital with the appropriate metal orbital should be little affected by the asymmetric disposition of the Ru atom with respect to the germylene moiety. In fact, the very low energy of the HOMO-86 orbital indicates that this overlap is quite efficient. It is also notable that germylene **1** does not behave as a π -acceptor ligand in complex **5**, since no bonding molecular orbitals displaying π -type overlaps between the Ge and Ru atoms have been found. The long Ru–Ge bond length (2.434(1) Å) should be a consequence of (a) the large contribution of the Ge 4s atomic orbital to the Ru–Ge bond (an hybrid sp^2 orbital would lead to a more efficient σ overlap than an s orbital) and (b) the absence of Ru to Ge π back-bonding.

Considering the possibility of inducing an intramolecular rearrangement of complex **5** involving the insertion of the

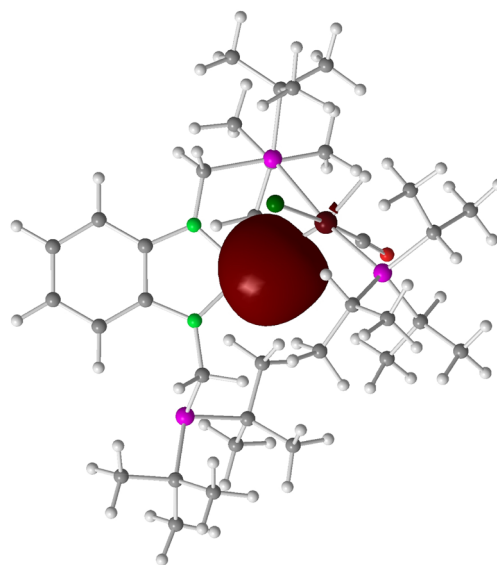


Figure 7. Principal molecular orbital (HOMO-86) responsible for the Ge–Ru bond of complex **5**. Its composition is 69.32% Ge (81.45% s, 18.54% p, 0.01% d) and 30.68% Ru (18.00% s, 61.00% p, 21.00% d).

germylene moiety of into the Ru–Cl or Ru–H bond, we heated at 100°C a toluene solution of complex **5**, but in all instances (various reaction times) we got a mixture of products (^{31}P NMR analysis) that we could not separate or characterize.

CONCLUDING REMARKS

An XRD study has established that the structure of the only hitherto known pincer-type diphosphane-germylene $\text{Ge}(\text{NCH}_2\text{P}^i\text{Bu}_2)_2\text{C}_6\text{H}_4$ (**1**) is that previously predicted by DFT methods,^{15,17} which indicated that the most stable conformation of the molecule has the lone pairs of both P atoms weakly interacting with empty orbitals mainly located on the Ge atom.

The isolation of compounds **2** and **4** has proven the propensity of the Ge atom of **1** to end inserted into inorganic σ bonds, such as Ir–Cl (**2**) and Mn–Mn (**4**). The chloridogermyl (**2**) and germylene (**4**) moieties of these reaction products are additionally attached to the metal atoms through one (**2**) or two (**4**) of their phosphane groups. The short distance found between the Ge atom and the pendant phosphane group P atom of complex **2** has been rationalized by DFT calculations. The synthesis of the trigonal-bipyramidal dicarbonyl derivative **3** demonstrates that the PGeP chloridogermyl ligand of complex **2** can also act as a P, Ge, P -tripodal ligand.

The reaction that led to complex **5**, in which germylene **1** is Ge, P -chelated to the ruthenium atom, is the first one to render a transition-metal derivative that does not arise from an insertion process but from a simple Ge, P -chelation of germylene **1** to a metal atom. In complex **5**, the short length of its coordinated $\text{CH}_2\text{P}^i\text{Pr}_2$ arm provokes the Ge atom to be in an uncommon T-shaped environment. A molecular orbital analysis of complex **5** has shown that the germylene moiety mainly uses its nondirectional Ge 4s orbital for the bonding with the Ru atom.

This contribution, in conjunction with previous papers dealing with the reactivity of the PGeP pincer-type germylene **1** with rhodium,¹⁵ cobalt,¹⁵ and group 10 metal complexes,¹⁶ helps demonstrate that transition-metal complexes containing PGeP pincer germyl or germylene ligands can be prepared

directly from the PGeP germylene, also opening up the possibility to explore in the near future the involvement of these complexes in catalytic adventures.

EXPERIMENTAL SECTION

General Procedures. Solvents were dried over appropriate desiccating reagents and were distilled under argon immediately before use. All reactions were carried out under argon in a dry glovebox or using either Schlenk or vacuum-line techniques. Published procedures were followed to prepare germylene **1**,¹⁵ $[\text{Ir}_2(\mu\text{-Cl})_2(\eta^4\text{-cod})_2]$,³⁰ and $[\text{RuHCl}(\text{CO})(\text{P}^i\text{Pr}_3)_2]$.³¹ All remaining reagents were purchased from commercial sources. The reaction products were vacuum-dried for several hours prior to being weighed and analyzed. IR spectra were recorded with a PerkinElmer Paragon 1000 spectrophotometer, using solution cells equipped with CaF_2 windows. NMR spectra were run on Bruker DPX-300 and NAV-400 instruments, using as standards the residual protic solvent resonance for ^1H ($\delta(\text{C}_6\text{HD}_5)$ 7.16 ppm; $\delta(\text{CHDCl}_2)$ 5.32 ppm), the solvent resonance for ^{13}C ($\delta(\text{C}_6\text{D}_6)$ 128.4 ppm; $\delta(\text{CD}_2\text{Cl}_2)$ 54.0 ppm), and aqueous 85% H_3PO_4 as an external reference for ^{31}P ($\delta(\text{H}_3\text{PO}_4)$ 0.0 ppm); ^{13}C assignments were done with the help of DEPT-135 spectra. Microanalyses were obtained with a PerkinElmer 2400 microanalyzer. Mass spectra (LRMS) were obtained with a Bruker Impact II mass spectrometer operating in the ESI-Q-ToF positive mode; data given refer to the most probable isotopomer.

$[\text{Ir}(\kappa^2\text{Ge,P-GeCl}(\text{NCH}_2\text{P}^i\text{Bu}_2)_2\text{C}_6\text{H}_4)(\eta^4\text{-cod})]$ (2**).** In a drybox, toluene (3 mL) was placed in a vial charged with germylene **1** (58 mg, 0.12 mmol) and $[\text{Ir}_2(\mu\text{-Cl})_2(\eta^4\text{-cod})_2]$ (40 mg, 0.06 mmol). The mixture was stirred at room temperature for 30 min. The initial orange color changed rapidly to dark red. The solvents were removed under reduced pressure, and the residue was washed with hexanes (5 mL) and vacuum-dried to give **2** as a red solid (80 mg, 82%). Anal. Calcd for $\text{C}_{32}\text{H}_{56}\text{ClIrN}_2\text{P}_2$ ($M_w = 831.05$ Da): C, 46.25; H, 6.79; N, 3.37. Found: C, 46.66; H, 6.82; N, 3.25. (+)-ESI LRMS: m/z found 859; calcd for $[\text{M} - \text{Cl} + 2 \text{ MeOH}]^+$ 859.33. ^1H NMR (CD_2Cl_2 , 300.1 MHz, 293 K): δ 6.75–6.60 (m, 4 H, 4 CH of C_6H_4), 5.29 (m, br, 2 H, 2 CH of cod), 5.19 (s, br, 2 H, 2 CH of cod), 3.72 (m, 1 H, 1 CH of PCH_2), 3.59 (m, 1 H, 1 CH of PCH_2), 3.29 (m, br, 1 CH of PCH_2), 3.06 (m, 1 H, 1 CH of PCH_2), 2.25–1.75 (m, br, 8 H of 4 CH_2 of cod), 1.38 (d, $J_{\text{HP}} = 11.6$ Hz, 9 H, 3 CH_3 of 'Bu), 1.29 (d, $J_{\text{HP}} = 12.1$ Hz, 9 H, 3 CH_3 of 'Bu), 1.19 (d, $J_{\text{HP}} = 12.2$ Hz, 9 H, 3 CH_3 of 'Bu), 1.13 (d, $J_{\text{HP}} = 10.7$ Hz, 9 H, 3 CH_3 of 'Bu), ppm. $^{13}\text{C}\{^1\text{H}\}$ NMR (CD_2Cl_2 , 100.6 MHz, 293 K): δ 143.9 (d, $J_{\text{CP}} = 1.4$ Hz, C of C_6H_4), 140.4 (d, $J_{\text{CP}} = 1.1$ Hz, C of C_6H_4), 117.5 (s, CH of C_6H_4), 116.8 (s, CH of C_6H_4), 109.5 (s, CH of C_6H_4), 108.8 (s, CH of C_6H_4), 81.5 (m, br, 4 CH of cod), 42.1 (d, $J_{\text{CP}} = 16.0$ Hz, 1 C of 'Bu), 38.8 (s, br, CH_2 of PCH_2), 36.6 (d, $J_{\text{CP}} = 14.6$ Hz, 1 C of 'Bu), 33.5 (d, $J_{\text{CP}} = 34.2$ Hz, CH_2 of PCH_2), 33.0–32.0 (m, 2 C of tBu + CH_2 of PCH_2 + 4 CH_2 of cod), 30.8–29.5 (m, 12 CH_3 of 4 'Bu) ppm. $^{31}\text{P}\{^1\text{H}\}$ NMR (C_6D_6 , 162.0 MHz, 293 K): δ 75.9 (s), 29.7 (s) ppm.

$[\text{Ir}(\kappa^3\text{P,Ge,P-GeCl}(\text{NCH}_2\text{P}^i\text{Bu}_2)_2\text{C}_6\text{H}_4)(\text{CO})_2]$ (3**).** In a Schlenk tube, carbon monoxide was bubbled for 10 min through a toluene (4 mL) solution of complex **3** (42 mg, 0.05 mmol). The color changed from dark orange to yellow. The resulting solution was evaporated to dryness to give **3** as a yellow solid (38 mg, 98%). Anal. Calcd for $\text{C}_{26}\text{H}_{44}\text{ClIrN}_2\text{O}_2\text{P}_2$ ($M_w = 778.88$ Da): C, 40.09; H, 5.69; N, 3.60. Found: C, 40.16; H, 5.77; N, 3.55. (+)-ESI LRMS: m/z found 751; calcd for $[\text{M} - \text{CO} + \text{H}]^+$ 751.15. IR (toluene): ν_{CO} 2001 (vs), 1956 (vs) cm^{-1} . ^1H NMR (C_6D_6 , 400.1 MHz, 293 K): δ 6.92 (m, 2 H, 2 CH of C_6H_4), 6.85 (m, 2 H, 2 CH of C_6H_4), 3.39 (m, 2 H, 2 CH of PCH_2), 2.95 (m, 2 H, 2 CH of PCH_2), 1.21 (m, 18 H, 6 CH_3 of 2 'Bu), 0.79 (m, 18 H, 6 CH_3 of 2 'Bu) ppm. $^{13}\text{C}\{^1\text{H}\}$ NMR (C_6D_6 , 100.6 MHz, 293 K): δ 187.1 (t, $J_{\text{CP}} = 9.1$ Hz, CO), 178.6 (t, $J_{\text{CP}} = 32.2$ Hz, CO), 146.8 (s, 2 C of C_6H_4), 120.0 (s, 2 CH of C_6H_4), 115.9 (s, 2 CH of C_6H_4), 49.0 (s, 2 CH_2 of 2 PCH_2), 38.7 (s, 2 C of 2 'Bu), 36.8 (s, 2 C of 2 'Bu), 30.4 (s, 6 CH_3 of 2 'Bu), 29.8 (s, 6 CH_3 of 2 'Bu) ppm. $^{31}\text{P}\{^1\text{H}\}$ NMR (C_6D_6 , 162.0 MHz, 293 K): δ 116.3 (s) ppm.

$[\text{Mn}_2(\mu\text{-}\kappa^3\text{P,Ge,P-Ge}(\text{NCH}_2\text{P}^i\text{Bu}_2)_2\text{C}_6\text{H}_4)(\text{CO})_8]$ (4**).** A Schlenk tube was charged with germylene **1** (40 mg, 0.08 mmol),

$[\text{Mn}_2(\text{CO})_{10}]$ (31 mg, 0.08 mmol), and toluene (5 mL). The yellow solution was stirred at reflux temperature for 4 h. The color changed from yellow to red-brown. A flash chromatographic separation (2×5 cm silica gel column packed in hexane), with dichloromethane as eluent, afforded compound **4** as a red solid (37 mg, 56%). Anal. Calcd for $\text{C}_{32}\text{H}_{44}\text{GeMn}_2\text{N}_2\text{O}_8\text{P}_2$ ($M_w = 829.15$ Da): C, 46.35; H, 5.35; N, 3.38. Found: C, 46.44; H, 5.47; N, 3.36. (+)-ESI LRMS: m/z found 830; calculated for $[\text{M}]^+$ 830.06. IR (toluene): ν_{CO} 2050 (m), 2021 (s), 1970 (sh), 1964 (s), 1947 (m), 1931 (s) cm^{-1} . ^1H NMR (C_6D_6 , 300.1 MHz, 293 K): δ 6.84 (m, 2 H, 2 CH of C_6H_4), 6.69 (m, 2 H, 2 CH of C_6H_4), 4.09 (dd, $J_{\text{HH}} = 14.1$ Hz, $J_{\text{HP}} = 8.4$ Hz, 2 H, 2 CH of PCH_2), 3.05 (dd, $J_{\text{HH}} = 14.1$ Hz, $J_{\text{HP}} = 10.3$ Hz, 2 H, 2 CH of PCH_2), 1.16 (d, $J_{\text{HP}} = 12.3$ Hz, 18 H, 6 CH_3 of 2 'Bu), 0.93 (d, $J_{\text{HP}} = 12.5$ Hz, 18 H, 6 CH_3 of 2 'Bu) ppm. $^{13}\text{C}\{^1\text{H}\}$ NMR (CD_2Cl_2 , 100.6 MHz, 293 K): δ 220.3–214.4 (m, COs), 146.7 (s, 2 C of C_6H_4), 116.5 (s, 2 CH of C_6H_4), 109.6 (s, 2 CH of C_6H_4), 41.6 (s, br, 2 CH_2 of 2 PCH_2), 37.7 (s, br, 4 C of 4 'Bu), 30.7 (s, 6 CH_3 of 2 'Bu), 30.3 (s, 6 CH_3 of 2 'Bu) ppm. $^{31}\text{P}\{^1\text{H}\}$ NMR (CD_2Cl_2 , 162.0 MHz, 293 K): δ 142.7 (s) ppm.

$[\text{RuHCl}(\text{CO})(\kappa^2\text{Ge,P-Ge}(\text{NCH}_2\text{P}^i\text{Bu}_2)_2\text{C}_6\text{H}_4)(\text{P}^i\text{Pr}_3)]$ (5**).** In a drybox, a vial was charged with germylene **1** (173 mg, 0.35 mmol), $[\text{RuHCl}(\text{CO})(\text{P}^i\text{Pr}_3)_2]$ (170 mg, 0.35 mmol), and toluene (3 mL). The yellow solution was stirred at room temperature for 1 h (no color change was observed) and was evaporated to dryness. The residue was washed with hexane (3×3 mL) and vacuum-dried to give **5** as a yellow solid (209 mg, 73%). Anal. Calcd for $\text{C}_{34}\text{H}_{66}\text{ClGeN}_2\text{OP}_3\text{Ru}$ ($M_w = 820.97$ Da): C, 49.74; H, 8.10; N, 3.41. Found: C, 49.93; H, 8.22; N, 3.36. ESI LRMS: no useful spectrum could be obtained. IR (toluene): ν_{CO} 1916 (s) cm^{-1} . ^1H NMR (C_6D_6 , 400.1 MHz, 293 K): δ 7.54 (m, 1 H, 1 CH of C_6H_4), 7.19–7.15 (m, 2 H, 2 CH of C_6H_4 , overlapped with the solvent peak), 7.05 (m, 1 H, 1 CH of C_6H_4), 4.35 (d, $J_{\text{HP}} = 14.2$ Hz, 1 H, 1 CH of PCH_2), 4.17–3.93 (m, 3 H, 3 CH of 2 PCH_2), 2.71 (m, 3 H, 3 CH of P^iPr_3), 1.56–1.36 (m, 30 H, 10 CH_3 of P^iPr_3 and 'Bu), 1.18–1.09 (m, 24 H, 8 CH_3 of P^iPr_3 and 'Bu), –8.73 (dd, $J_{\text{HP}} = 21.6$ and 16.3 Hz, 1 H, RuH) ppm. $^{13}\text{C}\{^1\text{H}\}$ NMR (C_6D_6 , 100.6 MHz, 293 K): δ 142.0 (s, C of C_6H_4), 141.7 (d, $J_{\text{C-P}} = 10.9$ Hz, C of C_6H_4), 119.5 (s, CH of C_6H_4), 117.8 (s, CH of C_6H_4), 111.8 (d, $J_{\text{CP}} = 7.5$ Hz, CH of C_6H_4), 109.9 (s, CH of C_6H_4), 42.7 (d, $J_{\text{CP}} = 22.4$ Hz, CH_2 of PCH_2), 37.8 (d, $J_{\text{CP}} = 15.7$ Hz, C of 'Bu), 37.4 (d, $J_{\text{CP}} = 11.8$ Hz, C of 'Bu), 33.4 (d, $J_{\text{CP}} = 23.8$ Hz, CH_2 of PCH_2), 32.4 (d, $J_{\text{CP}} = 10.1$ Hz, C of 'Bu), 32.2 (d, $J_{\text{CP}} = 11.4$ Hz, C of 'Bu), 31.5 (s, 3 CH_3 of 'Bu), 31.0 (s, 3 CH_3 of 'Bu), 30.2 (d, $J_{\text{CP}} = 12.9$ Hz, 3 CH_3 of P^iPr_3), 30.0 (d, $J_{\text{CP}} = 12.5$ Hz, 3 CH_3 of P^iPr_3), 24.3 (d, $J_{\text{CP}} = 20.2$ Hz, 3 CH of P^iPr_3), 20.4 (s, 3 CH_3 of 'Bu), 20.0 (s, 3 CH_3 of 'Bu) ppm. $^{31}\text{P}\{^1\text{H}\}$ NMR (C_6D_6 , 162.0 MHz, 293 K): δ 99.9 (d, $J_{\text{PP}} = 243.0$ Hz), 66.2 (d, $J_{\text{PP}} = 243.0$ Hz), 16.0 (s) ppm.

X-ray Diffraction Analyses. Crystals of **1**, **2**, **3**, **0.75C₇H₈**, **4**, **C₇H₈**, and **5** were analyzed by X-ray diffraction. They all were obtained in the drybox by slow evaporation of toluene solutions contained in open vials. A selection of crystal, measurement, and refinement data is given in Table S1. Diffraction data were collected on an Oxford Diffraction Xcalibur Onyx Nova single-crystal diffractometer with Cu $K\alpha$ radiation. Empirical absorption corrections were applied using the SCALE3 ABSPACK algorithm as implemented in CrysAlisPro RED.³² The structures were solved using SIR-97.³³ Isotropic and full matrix anisotropic least-squares refinements were carried out using SHELXL.³⁴ All non-H atoms were refined anisotropically. H atoms were set in calculated positions and were refined riding on their parent atoms. The position of the hydride ligand of **5** was calculated with XHYDEX.³⁵ The methyls of one *tert*-butyl group of **2** (C8 is its quaternary carbon) were disordered over two positions with a 68:32 occupancy ratio, requiring restraints on the geometrical and thermal parameters. The toluene solvent molecules found in the crystal of **3**·**0.75C₇H₈** were disordered about centers of symmetry and required restraints on their geometrical and thermal parameters. The WINGX program system³⁶ was used throughout the structure determinations. The molecular plots were made with MERCURY.³⁷ CCDC deposition numbers: 1829992 (**1**), 1829993 (**2**), 1829994 (**3**·**0.75C₇H₈**), 1829995 (**4**·**C₇H₈**), and 1829996 (**5**).

Theoretical Calculations. DFT calculations were carried out using the wB97XD functional,³⁸ which includes the second generation

of Grimme's dispersion interaction correction³⁹ as well as long-range interaction effects. This functional reproduces the local coordination geometry of transition-metal compounds very well, and it also corrects the systematic overestimation of nonbonded distances seen for all the density functionals that do not include estimates of dispersion.⁴⁰ The Stuttgart–Dresden relativistic effective core potential and the associated basis sets (SDD) were used for the Ir⁴¹ and Ru atoms.⁴² The basis set used for the remaining atoms was cc-pVDZ.⁴³ The stationary points were fully optimized in the gas phase and confirmed as energy minima (all positive eigenvalues) by analytical calculation of frequencies. The orbital analysis was carried out within the NBO framework.⁴⁴ All calculations were carried out with the Gaussian09 package.⁴⁵ The atomic coordinates of all the DFT-optimized structures are given in the [Supporting Information](#).

■ ASSOCIATED CONTENT

■ Supporting Information

The Supporting Information is available free of charge on the ACS Publications website at DOI: [10.1021/acs.organomet.8b00171](https://doi.org/10.1021/acs.organomet.8b00171).

¹H, ¹³C{¹H}, and ³¹P{¹H} NMR spectra of complexes 2–5 and crystal, measurement, and refinement data for the compounds studied by XRD (PDF)

Atomic coordinates for the DFT-optimized structures (XYZ)

Accession Codes

CCDC 1829992–1829996 contain the supplementary crystallographic data for this paper. These data can be obtained free of charge via www.ccdc.cam.ac.uk/data_request/cif, or by emailing data_request@ccdc.cam.ac.uk, or by contacting The Cambridge Crystallographic Data Centre, 12 Union Road, Cambridge CB2 1EZ, UK; fax: +44 1223 336033.

■ AUTHOR INFORMATION

Corresponding Author

*E-mail for J.A.C.: jac@uniovi.es.

ORCID

Javier A. Cabeza: 0000-0001-8563-9193

Notes

The authors declare no competing financial interest.

■ ACKNOWLEDGMENTS

This work has been supported by MINECO-FEDER (CTQ2016-75218-P, MAT2016-78155-C2-1-R, RYC2012-10491, and CTQ2016-81797-REDC) and Gobierno del Principado de Asturias (GRUPIN14-009 and GRUPIN14-060) research grants.

■ REFERENCES

- (1) Reviews on transition-metal chemistry of heavier tetrelenes: (a) Tacke, R.; Ribbeck, T. *Dalton Trans.* **2017**, 46, 13628–13659. (b) Cabeza, J. A.; García-Álvarez, P.; Polo, D. *Eur. J. Inorg. Chem.* **2016**, 2016, 10–22. (c) Álvarez-Rodríguez, L.; Cabeza, J. A.; García-Álvarez, P.; Polo, D. *Coord. Chem. Rev.* **2015**, 300, 1–28. (d) Blom, B.; Stoelzel, M.; Driess, M. *Chem. - Eur. J.* **2013**, 19, 40–62. (e) Baumgartner, J.; Marschner, C. *Rev. Inorg. Chem.* **2014**, 34, 119–152. (f) Zabula, A. V.; Hahn, F. E. *Eur. J. Inorg. Chem.* **2008**, 2008, 5165–5179. (g) Leung, W.-P.; Kan, K.-W.; Chong, K.-H. *Coord. Chem. Rev.* **2007**, 251, 2253–2265. (h) Waterman, R.; Hayes, P. G.; Tilley, T. D. *Acc. Chem. Res.* **2007**, 40, 712–719. (i) Köhl, O. *Coord. Chem. Rev.* **2004**, 248, 411–427. (j) Okazaki, M.; Tobita, H.; Ogino, H. *Dalton Trans.* **2003**, 493–506.
- (2) (a) Benedek, Z.; Szilvási, T. *Organometallics* **2017**, 36, 1591–1600. (b) Benedek, Z.; Szilvási, T. *RSC Adv.* **2015**, 5, 5077–5086.
- (c) Álvarez-Rodríguez, L.; Cabeza, J. A.; García-Álvarez, P.; Pérez-Carreño, E.; Polo, D. *Inorg. Chem.* **2015**, 54, 2983–2994. (d) Cabeza, J. A.; García-Álvarez, P.; Pérez-Carreño, E.; Polo, D. *Chem. - Eur. J.* **2014**, 20, 8654–8663.
- (3) Reviews on heavier tetrelenes as ligands in homogeneous catalysts: (a) Raoufmoghaddam, S.; Zhou, Y.-P.; Wang, Y.; Driess, M. *J. Organomet. Chem.* **2017**, 829, 2–10. (b) Blom, B.; Gallego, D.; Driess, M. *Inorg. Chem. Front.* **2014**, 1, 134–148.
- (4) Articles on nonpincer heavier tetrelenes as ligands in homogeneous catalysis not cited in ref 3: (a) Álvarez-Rodríguez, L.; Cabeza, J. A.; García-Álvarez, P.; Pérez-Carreño, E. *Organometallics* **2018**, DOI: [10.1021/acs.organomet.7b00905](https://doi.org/10.1021/acs.organomet.7b00905). (b) Schmidt, M.; Blom, B.; Szilvási, T.; Schomacker, R.; Driess, M. *Eur. J. Inorg. Chem.* **2017**, 2017, 1284–1291. (c) Iimura, T.; Akasaka, N.; Kosai, T.; Iwamoto, T. *Dalton Trans.* **2017**, 46, 8868–8874. (d) Iimura, T.; Akasaka, N.; Iwamoto, T. *Organometallics* **2016**, 35, 4071–4076. (e) Álvarez-Rodríguez, L.; Cabeza, J. A.; Fernández-Colinas, J. M.; García-Álvarez, P. *Organometallics* **2016**, 35, 2516–2523. (f) Zhou, Y.-P.; Raoufmoghaddam, S.; Szilvási, T.; Driess, M. *Angew. Chem., Int. Ed.* **2016**, 55, 12868–12872. (g) Xu, S.; Boschen, J. S.; Biswas, A.; Kobayashi, T.; Pruski, M.; Windus, T. L.; Sadow, A. D. *Dalton Trans.* **2015**, 44, 15897–15904. (h) Smart, K. A.; Mothes-Martin, E.; Vendier, L.; Perutz, R. N.; Grellier, M.; Sabo-Etienne, S. *Organometallics* **2015**, 34, 4158–4163. (i) Kireenko, M. M.; Zaitsev, K. V.; Oprunenko, Y. F.; Churakov, A. V.; Tafeenko, V. A.; Karlov, S. S.; Zaitseva, G. S. *Dalton Trans.* **2013**, 42, 7901–7912. (j) Fasulo, M. E.; Lipke, M. C.; Tilley, T. D. *Chem. Sci.* **2013**, 4, 3882–3887. (k) Calimano, E.; Tilley, T. D. *J. Am. Chem. Soc.* **2009**, 131, 11161–11173. (l) Calimano, E.; Tilley, T. D. *J. Am. Chem. Soc.* **2008**, 130, 9226–9227. (m) Waterman, R.; Hayes, P. G.; Tilley, T. D. *Acc. Chem. Res.* **2007**, 40, 712–719. (n) Glaser, P. B.; Tilley, T. D. *J. Am. Chem. Soc.* **2003**, 125, 13640–13641. (o) Litz, K. E.; Bender, J. E.; Kampf, J. W.; Holl, M. M. B. *Angew. Chem., Int. Ed. Engl.* **1997**, 36, 496–498.
- (5) Recent reviews on pincer complexes and their applications: (a) Peris, E.; Crabtree, R. H. *Chem. Soc. Rev.* **2018**, 47, 1959–1968. (b) Balakrishna, M. S. *Polyhedron* **2018**, 143, 2–10. (c) Maser, L.; Vondung, L.; Langer, R. *Polyhedron* **2018**, 143, 28–42. (d) Fernández-Álvarez, F. J.; Lalrempuia, R.; Oro, L. A. *Coord. Chem. Rev.* **2017**, 350, 49–60. (e) *The Privileged Pincer–Metal Platform: Coordination Chemistry & Applications*, van Koten, G., Gossage, R. A., Eds.; Springer: Cham, Switzerland, 2016. (f) Asay, M.; Morales-Morales, D. *Dalton Trans.* **2015**, 44, 17432–17447. (g) Gunanathan, C.; Milstein, D. *Chem. Rev.* **2014**, 114, 12024–12087. (h) *Organometallic Pincer Chemistry*; van Koten, G., Milstein, D., Eds.; Springer: Heidelberg, Germany, 2013. (i) Choi, J.; MacArthur, A. H. R.; Brookhart, M.; Goldman, A. S. *Chem. Rev.* **2011**, 111, 1761–1779. (j) Selander, N.; Szabó, K. J. *Chem. Rev.* **2011**, 111, 2048–2076. (k) *The Chemistry of Pincer Compounds*; Morales-Morales, D., Jensen, C., Eds.; Elsevier Science: Amsterdam, 2007. (l) Yamashita, M. *Bull. Chem. Soc. Jpn.* **2016**, 89, 269–281. (m) Turculet, L. In *The Chemistry of Pincer Compounds*; Szabó, K. J., Wendt, O. F., Eds.; Wiley-VCH: Weinheim, Germany, 2014; pp 149–187. (n) van der Vlugt, J. I. *Angew. Chem., Int. Ed.* **2010**, 49, 252–255. (o) Benito-Garagorri, D.; Kirchner, K. *Acc. Chem. Res.* **2008**, 41, 201–213. (p) Pugh, D.; Danopoulos, A. A. *Coord. Chem. Rev.* **2007**, 251, 610–641.
- (6) Recent reviews on pincer complexes in homogeneous catalysis: (a) Bauer, G.; Hu, X. *Inorg. Chem. Front.* **2016**, 3, 741–765. (b) Younus, H. A.; Su, W.; Ahmad, N.; Chen, S.; Verpoort, F. *Adv. Synth. Catal.* **2015**, 357, 283–330. (c) *Catalysis by Pincer Complexes: Applications in Organic Synthesis and Catalysis*; Szabó, K. J., Wendt, O. F., Eds.; Wiley-VCH: Weinheim, Germany, 2014. (d) Deng, Q.-H.; Melen, R. L.; Gade, L. H. *Acc. Chem. Res.* **2014**, 47, 3162–3173.
- (7) (a) Cabeza, J. A.; García-Álvarez, P.; González-Álvarez, L. *Chem. Commun.* **2017**, 53, 10275–10278. (b) Werner, H. *Angew. Chem., Int. Ed. Engl.* **1983**, 22, 927–949. (c) Collman, J. P.; Roper, W. R. *Adv. Organomet. Chem.* **1969**, 7, 53–94. (d) Vaska, L. *Acc. Chem. Res.* **1968**, 1, 335–344. (e) Shriver, D. F. *Acc. Chem. Res.* **1970**, 3, 231–238.
- (8) Hahn, F. E.; Zabula, A. V.; Pape, T.; Hepp, A. *Eur. J. Inorg. Chem.* **2007**, 2007, 2405–2408.

- (9) (a) Hahn, F. E.; Wittenbecher, L.; Kühn, M.; Lügger, T.; Fröhlich, R. J. *Organomet. Chem.* **2001**, 617–618, 629–634. (b) Hahn, F. E.; Wittenbecher, L.; Le Van, D.; Zabula, A. V. *Inorg. Chem.* **2007**, 46, 7662–7667.
- (10) (a) Brück, A.; Gallego, D.; Wang, W.; Irran, E.; Driess, M.; Hartwig, J. F. *Angew. Chem., Int. Ed.* **2012**, 51, 11478–11482. (b) Wang, W.; Inoue, S.; Irran, E.; Driess, M. *Angew. Chem., Int. Ed.* **2012**, 51, 3691–3694. (c) Gallego, D.; Brück, A.; Irran, E.; Meier, F.; Kaupp, F.; Driess, M. *J. Am. Chem. Soc.* **2013**, 135, 15617–15626.
- (11) (a) Ren, H.; Zhou, Y.-P.; Bai, Y.; Cui, C.; Driess, M. *Chem. - Eur. J.* **2017**, 23, 5663–5667. (b) Zhou, Y.-P.; Karni, M.; Yao, S.; Apeloig, Y.; Driess, M. *Angew. Chem., Int. Ed.* **2016**, 55, 15096–15099. (c) Metsänen, T. T.; Gallego, D.; Szilvási, T.; Driess, M.; Oestreich, M. *Chem. Sci.* **2015**, 6, 7143–7149. (d) Gallego, D.; Inoue, S.; Blom, B.; Driess, M. *Organometallics* **2014**, 33, 6885–6897.
- (12) Whited, M. T.; Zhang, J.; Ma, S.; Nguyen, B. D.; Janzen, D. E. *Dalton Trans.* **2017**, 46, 14757–14761.
- (13) DeMott, J. C.; Gu, W. X.; McCulloch, B. J.; Herbert, D. E.; Goshert, M. D.; Walensky, J. R.; Zhou, J.; Ozerov, O. V. *Organometallics* **2015**, 34, 3930–3933.
- (14) Handwerker, H.; Paul, M.; Blumel, J.; Zybill, C. *Angew. Chem., Int. Ed. Engl.* **1993**, 32, 1313–1315.
- (15) Álvarez-Rodríguez, L.; Brugos, J.; Cabeza, J. A.; García-Álvarez, P.; Pérez-Carreño, E.; Polo, D. *Chem. Commun.* **2017**, 53, 893–896.
- (16) Álvarez-Rodríguez, L.; Brugos, J.; Cabeza, J. A.; García-Álvarez, P.; Pérez-Carreño, E. *Chem. - Eur. J.* **2017**, 23, 15107–15115.
- (17) Brugos, J.; Cabeza, J. A.; García-Álvarez, P.; Pérez-Carreño, E.; Polo, D. *Dalton Trans.* **2018**, 47, 4534–4544.
- (18) Mantina, M.; Chamberlin, A. C.; Valero, R.; Cramer, C. J.; Truhlar, D. G. *J. Phys. Chem. A* **2009**, 113, 5806–5812.
- (19) For XRD-characterized iridium(I)–germyl complexes, see: (a) Kameo, H.; Ikeda, K.; Bourissou, D.; Sakaki, S.; Takemoto, S.; Nakazawa, H.; Matsuzaka, H. *Organometallics* **2016**, 35, 713–719. (b) Kameo, H.; Ishii, S.; Nakazawa, H. *Dalton Trans.* **2012**, 41, 11386–11392. (c) Kameo, H.; Ishii, S.; Nakazawa, H. *Dalton Trans.* **2012**, 41, 8290–8296. (d) Adams, R. D.; Trufan, E. *Organometallics* **2010**, 29, 4346–4353. (e) Allen, J. M.; Brennessel, W. W.; Buss, C. E.; Ellis, J. E.; Minyaev, M. E.; Pink, M.; Warnock, G. F.; Winzenburg, M. L.; Young, V. G., Jr. *Inorg. Chem.* **2001**, 40, 5279–5284.
- (20) Hawkins, S. M.; Hitchcock, P. B.; Lappert, M. F.; Rai, A. K. *J. Chem. Soc., Chem. Commun.* **1986**, 1689–1690.
- (21) Whited, M. T.; Deetz, A. M.; Boerma, J. W.; DeRosha, D. E.; Janzen, D. E. *Organometallics* **2014**, 33, 5070–5073.
- (22) (a) Job, R. C.; Curtis, M. D. *Inorg. Chem.* **1973**, 12, 2514–2519. (b) Lei, D.; Hampden-Smith, M. J.; Duesler, E. N.; Huffman, J. C. *Inorg. Chem.* **1990**, 29, 795–798. (c) Herrmann, W. A.; Kneuper, H.-J.; Herdtweck, E. *Chem. Ber.* **1989**, 122, 433–436. (d) Ismail, M. L. B.; Liu, F.-Q.; Yim, W.-L.; Ganguly, R.; Li, Y.; So, C. W. *Inorg. Chem.* **2017**, 56, 5402–5410.
- (23) Veith, M.; Stahl, L.; Huch, V. *Organometallics* **1993**, 12, 1914–1920.
- (24) See, for example: (a) Esteruelas, M. A.; Herrero, J.; Oro, L. A. *Organometallics* **1993**, 12, 2377–2379. (b) Esteruelas, M. A.; Gómez, A. V.; Lahoz, F. J.; López, A. M.; Oñate, E.; Oro, L. A. *Organometallics* **1996**, 15, 3423–3425.
- (25) Herrmann, R.; Braun, T.; Mebs, S. *Eur. J. Inorg. Chem.* **2014**, 2014, 4826–4835.
- (26) Filippou, A. C.; Weidemann, N.; Philippopoulos, A. I.; Schnakenburg, G. *Angew. Chem., Int. Ed.* **2006**, 45, 5987–5991.
- (27) Hupp, F.; Ma, M.; Kroll, F.; Jiménez-Halla, J. O. C.; Dewhurst, R. D.; Radacki, K.; Stasch, A.; Jones, C.; Braunschweig, H. *Chem. - Eur. J.* **2014**, 20, 16888–16898.
- (28) (a) Cabeza, J. A.; Fernández-Colinas, J. M.; García-Álvarez, P.; Polo, D. *Inorg. Chem.* **2012**, 51, 3896–3903. (b) York, J. T.; Young, V. G.; Tolman, W. B. *Inorg. Chem.* **2006**, 45, 4191–4198. (c) Cygan, Z. T.; Bender, J. E., IV; Litz, K. E.; Kampf, J. W.; Holl, M. M. B. *Organometallics* **2002**, 21, 5373–5381. (d) Litz, K. E.; Bender, J. E., IV; Kampf, J. W.; Holl, M. M. B. *Angew. Chem., Int. Ed. Engl.* **1997**, 36, 496–498. (e) Litz, K. E.; Henderson, K.; Gourley, R. W.; Holl, M. M. B. *Organometallics* **1995**, 14, 5008–5010.
- (29) (a) Herrmann, W. A.; Denk, M.; Behm, J.; Scherer, W.; Klingan, F.-R.; Bock, H.; Solouki, B.; Wagner, M. *Angew. Chem., Int. Ed. Engl.* **1992**, 31, 1485–1488. (b) Ullah, F.; Köhl, O.; Bajor, G.; Veszpremi, T.; Jones, P. G.; Heinicke, J. *Eur. J. Inorg. Chem.* **2009**, 2009, 221–229. (c) Bazinet, P.; Yap, G. P. A.; Richeson, D. S. *J. Am. Chem. Soc.* **2001**, 123, 11162–11167. (d) Hahn, F. E.; Zabula, A. V.; Pape, T.; Hepp, A. Z. *Anorg. Allg. Chem.* **2008**, 634, 2397–2401. (e) Köhl, O.; Lönnecke, P.; Heinicke, J. *Inorg. Chem.* **2003**, 42, 2836–2838. (f) Veith, M.; Müller, A.; Stahl, L.; Notzel, M.; Jarczyk, M.; Huch, V. *Inorg. Chem.* **1996**, 35, 3848–3855. (g) Walz, F.; Moos, E.; Garnier, D.; Koppe, R.; Anson, C. E.; Breher, F. *Chem. - Eur. J.* **2017**, 23, 1173–1186. (h) Veith, M.; Stahl, L. *Angew. Chem., Int. Ed. Engl.* **1993**, 32, 106–107. (i) Zabula, A. V.; Hahn, F. E.; Pape, T.; Hepp, A. *Organometallics* **2007**, 26, 1972–1980.
- (30) Herde, J. L.; Lambert, J. C.; Senoff, C. V.; Cushing, M. A. *Inorg. Synth* **2007**, 15, 18–20.
- (31) Esteruelas, M. A.; Werner, H. *J. Organomet. Chem.* **1986**, 303, 221–231.
- (32) CrysAlisPro RED, version 1.171.38.46; Oxford Diffraction Ltd.: Oxford, U.K., 2015.
- (33) SIR-97: Altomare, A.; Burla, M. C.; Camalli, M.; Casciarano, G.; Giacovazzo, C.; Guagliardi, A.; Moliterni, A. G. C.; Polidori, G.; Spagna, R. *J. Appl. Crystallogr.* **1999**, 32, 115–119.
- (34) SHELXL-2014: Sheldrick, G. M. *Acta Crystallogr., Sect. A: Found. Crystallogr.* **2008**, 64, 112–122.
- (35) XHYDEX: Orpen, A. G. *J. Chem. Soc., Dalton Trans.* **1980**, 2509–2516.
- (36) Farrugia, L. J. *J. Appl. Crystallogr.* **2012**, 45, 849–854.
- (37) MERCURY, CSD 3.9 (build RC1); Cambridge Crystallographic Data Centre: Cambridge, U.K., 2016.
- (38) Chai, J.-D.; Head-Gordon, M. *Phys. Chem. Chem. Phys.* **2008**, 10, 6615–6620.
- (39) (a) Ehrlich, S.; Moellmann, J.; Grimme, S. *Acc. Chem. Res.* **2013**, 46, 916–926. (b) Grimme, S. *Comp. Mol. Sci.* **2011**, 1, 211–218. (c) Schwabe, T.; Grimme, S. *Acc. Chem. Res.* **2008**, 41, 569–579.
- (40) Minenkov, Y.; Singstad, Å.; Occhipinti, G.; Jensen, V. R. *Dalton Trans.* **2012**, 41, 5526–5541.
- (41) Figgen, D.; Peterson, K. A.; Dolg, M.; Stoll, H. *J. Chem. Phys.* **2009**, 130, 164108–164120.
- (42) Peterson, K. A.; Figgen, D.; Dolg, M.; Stoll, H. *J. Chem. Phys.* **2007**, 126, 124101–124112.
- (43) Dunning, T. H. *J. Chem. Phys.* **1989**, 90, 1007–1023.
- (44) Glendening, E. D.; Reed, A. E.; Carpenter, J. E.; Weinhold, F. *NBO 3.1*; Theoretical Chemistry Institute, University of Wisconsin: Madison, WI, 2002.
- (45) Frisch, M. J.; Trucks, G. W.; Schlegel, H. B.; Scuseria, G. E.; Robb, M. A.; Cheeseman, J. R.; Scalmani, G.; Barone, V.; Mennucci, B.; Petersson, G. A.; Nakatsuji, H.; Caricato, M.; Li, X.; Hratchian, H. P.; Izmaylov, A. F.; Bloino, J.; Zheng, G.; Sonnenberg, J. L.; Hada, M.; Ehara, M.; Toyota, K.; Fukuda, R.; Hasegawa, J.; Ishida, M.; Nakajima, T.; Honda, Y.; Kitao, O.; Nakai, H.; Vreven, T.; Montgomery, J. A., Jr.; Peralta, J. E.; Ogliaro, F.; Bearpark, M.; Heyd, J. J.; Brothers, E.; Kudin, K. N.; Staroverov, V. N.; Kobayashi, R.; Normand, J.; Raghavachari, K.; Rendell, A.; Burant, J. C.; Iyengar, S. S.; Tomasi, J.; Cossi, M.; Rega, N.; Millam, J. M.; Klene, M.; Knox, J. E.; Cross, J. B.; Bakken, V.; Adamo, C.; Jaramillo, J.; Gomperts, R.; Stratmann, R. E.; Yazyev, O.; Austin, A. J.; Cammi, R.; Pomelli, C.; Ochterski, J. W.; Martin, R. L.; Morokuma, K.; Zakrzewski, V. G.; Voith, G. A.; Salvador, P.; Dannenberg, J. J.; Dapprich, S.; Daniels, A. D.; Farkas, O.; Foresman, J. B.; Ortiz, J. V.; Cioslowski, J.; Fox, D. J. *Gaussian 09, revision A.01*; Gaussian, Inc.: Wallingford, CT, 2009.